Catalysis Today 181 (2012) 40–51

Contents lists available at SciVerse ScienceDirect

Catalysis Today

journal homepage: www.elsevier.com/locate/cattod

Influence of the catalyst loading on the activity and the CO selectivity of supported Ru catalysts in the selective methanation of CO in CO_2 containing feed gases

Stephan Eckle[a], Matthias Augustin[a], Hans-Georg Anfang[b], R. Jürgen Behm[a,*]

[a] Institute of Surface Chemistry and Catalysis, Ulm University, D-89069 Ulm, Germany
[b] Süd-Chemie AG, R&D Energy & Environment, Waldheimer Str. 13, D-83502 Bruckmühl, Germany

ARTICLE INFO

Article history:
Received 28 February 2011
Received in revised form 9 August 2011
Accepted 17 August 2011
Available online 23 September 2011

Keywords:
CO methanation
CO_2 methanation
Mechanism
CO adsorption
Selectivity
Ru catalyst

ABSTRACT

We have investigated the methanation of CO and CO_2 over Ru/zeolite catalysts with different Ru loading in semi-realistic reformate gases by *in situ* X-ray absorption spectroscopy (XAS), *in situ* diffuse reflectance infrared Fourier transform spectroscopy (DRIFTS) and kinetic measurements. Increasing the Ru loading causes an increase of the mean particle size from 0.9 nm (2.2 wt.% Ru) to 1.9 nm (5.6 wt.% Ru). At the same time, also the activity for CO methanation increases, while the selectivity for CO methanation, which is constant at 100% for reformate gases with 0.6% CO, decreases at low CO contents. The latter findings are interpreted in terms of a change in the physical effects governing the selectivity for CO methanation with increasing Ru particle size, from an inherently low activity for CO_2 dissociation and subsequent CO_{ad} methanation on very small Ru nanoparticles to a site blocking mechanism on larger Ru nanoparticles. In the latter mechanism, CO_2 methanation is hindered by a reaction inhibiting adlayer of CO at higher CO_{ad} coverages, i.e., at not too low CO concentrations, but facile in the absence of a CO adlayer, at lower CO concentrations in the reaction gas mixture.

1. Introduction

The methanation of CO has attracted increasing interest in recent years because of its potential as simple technique for CO removal from H_2-rich feed gases for low temperature fuel cells produced by steam reforming of fossil fuels or biomass based fuels [1]. It is an attractive alternative to the more commonly used selective CO oxidation (PROX) reaction in cost sensitive small scale applications, since it avoids the controlled addition of a second gas (O_2). Since the resulting reformates typically contain also considerable amounts of CO_2 (15–20%) [1–5], the reaction must be highly selective for CO methanation, with CO_2 methanation essentially being inhibited, otherwise the losses of H_2 would become intolerable [1,6]. Therefore, the mechanisms of these reactions, CO methanation and CO_2 methanation, as well the physical effects controlling the selectivity for the selective methanation of CO in CO_2-rich gas mixtures, are of obvious importance for industrial applications.

In addition to the commonly used Ni, Fe or Co-based catalysts for the Fischer-Tropsch reaction, also supported Ru catalysts are highly active for CO methanation [7–10]. For supported Ru catalysts, it was established in a number of studies that in addition to the nature of the support material, such as Al_2O_3, TiO_2 or zeolites, the Ru particle size has a pronounced effect on their activity for CO methanation [11–14]. The Ru mass normalized reaction rate was found to increase with increasing Ru particle size. For very small Ru nanoparticles with diameters <1 nm, the activity decreased steeply. This was associated with the higher fraction of Ru terrace sites on larger Ru nanoparticles, which were considered to be more active for this reaction [11–14]. While the above studies were conducted under Fischer-Tropsch reaction conditions in a typical syngas mixture (H_2:CO = 3), this trend was confirmed also in more recent studies performed under conditions more relevant for feed gas processing (H_2:CO = 14) [10,15,16].

The selectivity for CO methanation in the selective methanation of CO_2-rich gas mixtures was attributed to surface blocking by adsorbed CO, due to the much higher adsorption energy of CO compared to CO_2. The CO adlayer was proposed to inhibit the (dissociative) adsorption of CO_2 and thus the subsequent methanation reaction [17,18]. In that mechanism, CO_2 methanation will be inhibited as long as the CO partial pressure is sufficiently high to maintain the reaction inhibiting CO adlayer. Increasing the selectivity and activity of Ru supported catalysts has already been tried in many different ways, including the use of different support materials such as TiO_2, Al_2O_3, SiO_2 [16,19], or of dopants [20,21], or by varying the Ru particle size [22]. In the latter study on Ru/Al_2O_3 catalysts, the Ru particle sizes were varied between 7.5 and 34 nm, and a decrease in

* Corresponding author.
E-mail address: juergen.behm@uni-ulm.de (R.J. Behm).

0920-5861/$ – see front matter © 2011 Elsevier B.V. All rights reserved.
doi:10.1016/j.cattod.2011.08.035

the temperature for maximum methane formation with decreasing particle size was reported. Also the use of zeolite supports was proposed as an alternative to standard supports such as TiO_2 or Al_2O_3; the zeolite supported Ru catalysts showed indeed a higher selectivity for the methanation of CO compared to Ru/Al_2O_3 or Ru/SiO_2 catalysts [23,24]. This was explained by a stronger metal-support interaction.

Recently, we reported on a zeolite supported, commercial Ru catalyst, which showed an extremely high selectivity, essentially 100%, over a wide range of CO concentrations [25–27]. We could demonstrate that for a 2.2 wt.% Ru/zeolite catalyst this selectivity was maintained even in reaction gases with a very low CO content (100 ppm), where the CO_{ad} coverage on the Ru nanoparticles (NPs) was far below saturation. Moreover, this catalyst shows 100% CO selectivity and full CO conversion at 190 °C even under integral reaction conditions. CO_2 is methanated only at higher temperatures and exhibits 50% conversion at 350 °C [26]. In contrast, on a 5 wt.% Ru/Al_2O_3 catalyst, which was investigated for comparison, the selectivity decayed rapidly once the CO_{ad} coverage, as detected by its IR signal intensity, fell significantly below its saturation value [26]. This was tentatively attributed to an inherently low activity of the very small Ru NPs in the Ru/zeolite catalyst for CO_2 dissociation, which results in very low CO_2 methanation rates even at low CO_{ad} coverages, while on the Ru/Al_2O_3 catalyst with its much larger Ru particles (mean particle size around 2.5 nm), the inherent activity for CO_2 decomposition and methanation is quite high and high selectivities are only obtained by surface blocking by CO_{ad}. In that picture, the selectivity was primarily attributed to the Ru particle size, hence, to a particle size effect. This explanation, though convincing, was preliminary, since the Ru particle size in the Ru/zeolite catalysts was unknown. The Ru particles appeared to be too small for transmission electron microscopy (TEM) imaging and X-ray diffraction (XRD). Furthermore, since catalysts with two different supports were compared, support effects on the selectivity, due to metal-support interactions, cannot be ruled out.

These open questions are addressed in the present paper, where we report results of a systematic, combined kinetic and *in situ* spectroscopy study on the effect of Ru metal loading and Ru particle size on the activity and in particular on the selectivity of Ru/zeolite catalysts in the selective methanation of CO. The measurements were performed in a number of different idealized (H_2/CO, H_2/CO_2) and semi-realistic ($H_2/CO/CO_2$) reaction atmospheres, decreasing the CO content to as low as 100 ppm. *In situ* extended X ray absorption fine structure spectroscopy (EXAFS) and *in situ* diffuse reflectance IR spectroscopy (DRIFTS) measurements were employed, in addition to kinetic measurements, in order to gain information on the Ru particle sizes of the different catalysts during reaction under steady-state conditions (EXAFS) and on the temporal evolution of the adsorbate layer during the reaction (time-resolved DRIFTS). *In situ* EXAFS results, obtained after equilibration in idealized reformate (Table 1), are presented and discussed in Section 3.1. The time-resolved *in situ* DRIFTS measurements and their results are described in Section 3.2. In combination, the DRIFTS measurements allow us to not only determine the steady-state CO_{ad} coverages in the respective reaction atmospheres, but also to qualitatively assess the contribution from CO_2 decomposition to the CO_{ad} signal in semi-realistic reaction gases. The influence of the Ru loading and Ru particle size on the CO methanation activity and on the selectivity for CO methanation is topic of the following Section 3.3. The resulting correlations between CO_{ad} coverage and the selectivity for CO methanation and Ru particle size effects therein as well as consequences on the molecular scale mechanism responsible for the selectivity are discussed. Finally, we briefly comment on consequences of these findings for technical applications.

2. Experimental

Catalyst properties: The Ru/zeolite catalysts with metal loadings of 1, 2.2, 3.6, and 5.6 wt.% Ru were prepared by Süd-Chemie AG. BET specific surface areas of ~410 $m^2\,g^{-1}$ for the Ru/zeolite catalysts were determined by N_2 adsorption, and the catalysts were free of additional dopants. Reliable Ru particle size determination of the zeolite supported catalysts had turned out to be problematic both for standard techniques such as TEM or XRD for structure determination (structure) and also for H_2 chemisorption, where only upper limits of the particle size could be estimated [26]. Hence, this question is still open. Further details of the catalyst characterization are given elsewhere [26].

XAS experiments: The EXAFS experiments were performed at the X1 beamline at Hasylab and BM26 at ESRF, using a Si-311 double crystal monochromator and a beam size of approximately 6 mm vertical and 2 mm horizontal. The reaction cell consisted of a stainless steel ring with a cylindrical channel (i.d. 4 mm) along the diameter, which contained the catalyst bed (length ca. 10 mm, ~25 mg catalyst, undiluted, conversion <15%). A second bore, along the central axis of the ring and perpendicular to the catalyst bed, allowed the X-ray beam to pass through the catalyst bed. In these directions, the reaction cell was closed by two Kapton windows. Sample heating was achieved by 4 wires, which passed through the ring in 4 small bores parallel to the reaction channel. A NiCr/Ni thermocouple was used to monitor the temperature. The reaction cell was placed between two He filled ionization chambers for collecting the spectra at the Ru K-edge (22,117 eV) in transmission geometry. A Ru metal foil placed in between the second and a subsequent third ionization chamber allowed for internal energy calibration during all measurements. The pre-edge region was measured from 21,867 to 22,087, the XANES region from 22,087 to 22,157 eV (XANES data not shown), and the EXAFS region from 22,157 to 23,317 eV. Processing of the EXAFS spectra followed standard procedures [28], using the program 'XDAP' [29]. In short, the spectra were pre-edge and background subtracted using a modified Victoreen function and a spline function, respectively. Normalization for constant signal intensity of the spectra was performed 50 eV above the edge. Multiple shell fitting of the EXAFS was done in r-space ($3.2 < k < 13.5\ A^{-1}$, $1.0 < r < 3.2$), using a k weighting of 3. Theoretical references were calculated by FEFF 8.0 [30] and calibrated against a Ru foil and RuO_2 as experimental references, to obtain the damping factor S_0^2, the phase shift F and the mean free path of the electrons δ [28].

These *in situ* measurements were conducted with high purity gases (99.999%), which were passed through the reaction cell (gas flow 41.6 Nml min^{-1}). The reaction gas mixtures were prepared via mass flow controllers (Bronkhorst F201C-FA-88V). Prior to the *in situ* experiments, the catalysts were heated up in a N_2 stream to 150 °C, and subsequently heated within 10 min to the reaction temperature in the reaction gas atmosphere. The *in situ* EXAFS measurements were performed at 190 °C reaction temperature in idealized reformate at atmospheric pressure (0.6% CO, 3% N_2, balance H_2), until steady-state conditions were achieved, but at least for 500 min time on stream (max. 1000 min).

Kinetic measurements: The kinetic measurements were carried out at atmospheric pressure in a quartz tube micro reactor with the catalysts used as received. By diluting the catalyst with different amounts of SiO_2 (inactive under our reaction conditions), differential reaction conditions (maximum 15% conversion of the reactants) were obtained. The dilution of the catalyst with SiO_2 depended on the CO concentration and on the catalyst (0.6% CO: 1:5 (1 wt.% Ru/zeolite catalyst), 1:10 (2.2 wt:%), 1:30 (3.6 wt.%), 1:60 (5.6 wt.%); 100 ppm CO: 1:400 (3.6 wt.%) 1:600 (5.6 wt.%). In total, about 200 mg of diluted catalyst was used, resulting in a catalyst bed of 1 cm length. The experiments were carried out in a gas flow

Table 1
Composition of the different reformate gases used in the DRIFTS and kinetic measurements.

Reaction gas	Reaction gas composition		
	Fixed contents	CO content	CO_2 content
ID-ref 100: Low-CO idealized reformate (100 ppm CO)	2.8% N_2, balance H_2	100 ppm	0%
SR-ref 100: Low-CO semi-realistic reformate (100 ppm CO)	2.8% N_2, balance H_2	100 ppm	15.5%
SR–ref 6000: Semi-realistic reformate (6000 ppm CO)	2.8% N_2, balance H_2	6000 ppm	15.5%
CO_2-ref: CO_2 reformate (CO-free)	2.8% N_2, balance H_2	0 ppm	15.5%

of 41.6 Nml min^{-1} in the different gas mixtures (compositions see Table 1). Since the dimensions of the catalyst bed did not change significantly, the space velocity referenced to the total catalyst bed can be assumed as constant (5000 h^{-1}). Prior to the experiments, the catalysts were heated up in a N_2 stream to 150 °C, identical to the activation procedure in the *in situ* EXAFS measurements. Subsequently, the catalysts were heated within 10 min to the reaction temperature in reaction gas. The reaction/deactivation measurements were performed at 190 °C reaction temperature, following the reaction rate over 1000 min. The gas mixtures were prepared via mass flow controllers (Hastings HFC-202 and Bronkhorst F201C-FA-88V). Incoming and effluent gases were analyzed by on-line gas chromatography with a CO detection limit of ca. 10 ppm (DANI 86.10), using H_2 as carrier gas. Further details can be found in Ref. [25].

In situ IR spectroscopy measurements: In situ diffuse reflectance FTIR spectroscopy (DRIFTS) measurements were performed using a commercial *in situ* reaction cell (Harricks, HV-DR2) operated with continuous reaction gas flow. The spectra were recorded in a Magna 6700 spectrometer (Thermo) equipped with a MCT narrow-band detector. Around 30 mg of diluted catalyst (1:5 with α-Al_2O_3), placed on top of a 70 mg α-Al_2O_3 layer, were used as catalyst bed. The catalyst were pre-treated as described above, the background spectra were recorded at 150 °C, before admitting the reaction gas. During the reaction experiments, 400 scans were co-added for one spectrum. The intensities were evaluated in Kubelka–Munk units, which are linearly related to the adsorbate concentration [31] (for exceptions see [32]). Background subtraction and normalization of the spectra were performed by subtracting spectra recorded in a flow of N_2 directly after catalyst conditioning. For presentation, the spectra are split into 3 frequency ranges, the regions of the OH (3900–3400 cm^{-1}, top left) and CH_x (3250–2800 cm^{-1}, top right) stretch vibrations in the top panels, respectively, and the spectral range between 2200 and 1000 cm^{-1} including the CO stretch (2200–1900 cm^{-1}) and the OCO bending (1600–800 cm^{-1}) vibrations in the bottom panel. The spectra in the OH region are shown as raw data, since the significant change in the background intensity in this region with time did not allow us to determine appropriate background signals for the background subtraction.

3. Results and discussion

3.1. Ru particle sizes

The mean particle size of the Ru/zeolite catalysts was investigated by *in situ* EXAFS measurements, after previous attempts to derive the Ru particle size in a 2.2 wt.% Ru/zeolite catalyst by standard techniques for particle size determination (XRD, TEM) were unsuccessful because of the too low size of the Ru particles and because of electron beam induced decomposition of the zeolite support [25]. *In situ* EXAFS measurements were conducted in idealized reformate gas (ID-ref 6000), until the coordination number did not change any more, at least over 500 min.

The k^3 weighted chi functions obtained on the 2.2, 3.6 and 5.6 wt.% Ru/zeolite catalysts are plotted in the *k*-range from 3.2 to 13.0 A^{-1} in the left panels in Fig. 1. Measurements on the 1 wt.% Ru/zeolite catalyst could not be evaluated reliably, as the catalyst loading was too low to obtain a good quality spectrum. The right panels show the resulting Fourier transforms in r-space (Ru–Ru scattering, *r*-range: 1.0–6.0). It is clear that with higher loading and larger particles, respectively, the signal intensities in both *k* and *r*-space increase. The prominent signal (Ru–Ru scattering) at ~2.7 Å in *r*-space indicates that the particles are essentially metallic particles under steady-state conditions. It should be noted that the spectra could be fitted with only a single Ru–Ru shell. The result of metallic Ru NPs is compatible with previous findings in *in situ* DRIFTS measurements, which yielded vibrational frequencies for adsorbed CO similar to those characteristic for CO_{ad} on metallic Ru [25,26]. It should be noted that EXAFS spectra recorded prior to the experiment revealed that in this state the Ru NPs of all catalysts are oxidic, as indicated by the intense white line, which is similar to that of a RuO_2 reference compound, and the Ru–O spacing of 1.97 Å (see supporting information). They are reduced within 2 min after exposure to the reaction atmosphere, which from experimental reasons was not accessible to time-resolved measurements. In addition to the prominent peak of the first shell (~2.7 Å, Ru–Ru scattering), significantly smaller signals can also be observed at larger distances (~3.8 Å and ~4.7 Å) corresponding to 2nd and 3rd shell Ru–Ru scattering. These signals may indicate the presences of larger particles (see also below), which will contribute to the first and to higher shell signals and are probably located on the outer surface of the zeolite support [33].

The Ru–Ru coordination number, which was obtained by fitting the first shell (Ru–Ru at ~2.7 A) to the Ru foil reference (see Fig. 1), can be directly correlated to the mean particle size of the Ru NPs by using a relation determined by Karim et al. [34]. The dispersion ($D = N_{surf.}/N_{bulk}$) and the Ru surface area of the catalysts were calculated by assuming hemispherical Ru nanoparticles. Table 2 summarizes the structural parameters resulting from the fitting procedure. The 'goodness of the fit' was always between 1 and 2, indicative of a good fit. In addition, the coordination numbers did not change significantly when applying different *k* weightings, underlining the quality of the fits. The spectra taken at reaction temperature (190 °C) show a slightly smaller Ru–Ru bond length of ~2.67 Å compared to 2.70 Å in bulk Ru for all catalysts investigated, indicative of a contraction of the Ru lattice in the very small Ru NPs.

In contrast to the constant Ru–Ru bond length, the Ru coordination number increases with increasing catalyst loading, from 6.7 to 8.6 (Table 2), indicative of an increasing mean Ru particle size. This corresponds to particle sizes between 0.9 nm (2.2 wt.%) and 1.9 nm (5.6 wt.%). The very small Ru particle size obtained from EXAFS for the 2.2 wt.% Ru/zeolite catalyst supports our earlier proposal according to which most of the Ru NPs of the 2.2 wt.% Ru/zeolite catalyst are located in the pores of the zeolite [26]. This was based on the observation that in previous X-ray photoemission spectroscopy (XPS) measurements the intensity of the Ru(3d) signal on the 2.2 wt.% Ru/zeolite catalyst was only 5% of that on a non porous 5 wt.% Ru/Al_2O_3 catalyst, where the Ru NPs are deposited on the surface [26]. As mentioned before, we assume that in addition to the very small Ru NPs proposed to be located in the pores (0.8–0.9 nm) of the zeolite, also few larger Ru NPs are present on

Table 2
Results of the EXAFS fit procedure and resulting structural parameters of the different Ru/zeolites catalysts measured under steady-state conditions in idealized reformate (0.6% CO, balance H_2).

Catalyst	Coordination number	Debye Waller factor/10^{-3} Å^2	Distance/Å	E_0/eV	Mean Ru particle size/nm
2.2 wt.%	6.71 ± 0.21	6.62 ± 0.41	2.711 ± 0.007	6.12 ± 0.22	0.9
3.6 wt.%	8.31 ± 0.24	7.71 ± 0.42	2.673 ± 0.007	7.11 ± 0.21	1.6
5.6 wt.%	8.60 ± 0.23	6.83 ± 0.36	2.671 ± 0.003	8.02 ± 0.16	1.9

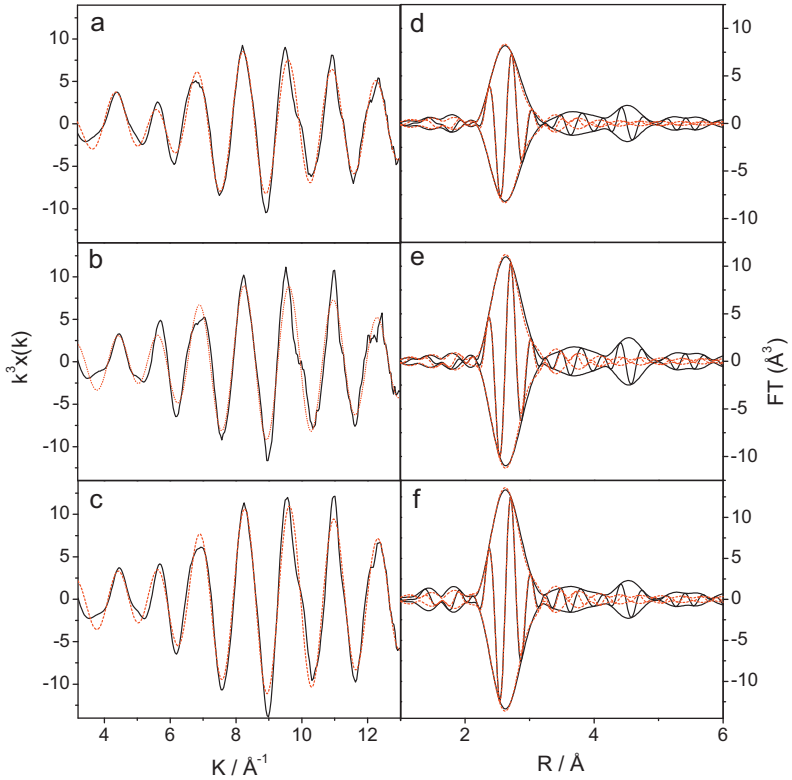

Fig. 1. Left: k^3 weighted chi function, right: corresponding Fourier transform (k^3-weighted, $3.2 < k < 13.0$ Å^{-1}) of (a, d) 2.2 wt.% Ru/zeolite, (b, e) 3.6 wt.% Ru/zeolite, (c, f) 5.6 wt.% Ru/zeolite.

the outer surface. Their number, however, must be rather small on the 2.2 wt.% catalyst. For the catalysts with higher Ru loading, the 3.6 and 5.6 wt.% Ru/zeolite catalysts, we tentatively suggest that the larger mean particle sizes obtained from the EXAFS measurements (1.6 and 1.9 nm, respectively) result from a higher fraction of larger particles, in addition to the very small Ru NPs in the pores of the zeolite.

In semi-realistic reformate (SR-ref 6000), containing 15.5% CO_2 in addition to 6000 ppm CO, we expect similar Ru particle sizes as determined in idealized reformate, since CO_{ad} will block the surface and hence the active sites for CO_2 dissociation and methanation. Therefore, the presence of CO_2 is not expected to measurably affect the Ru particle size.

3.2. *In-situ DRIFTS measurements*

The interaction of the different reaction atmospheres with the differently loaded Ru/zeolite catalysts and the resulting adlayer build-up were characterized by sequences of *in situ* DRIFT spectra, which were recorded over 1000 min on stream. The measurements were performed in different reaction atmospheres, including semi-realistic reformates (SR-ref 6000 and SR-ref 100), idealized reaction atmosphere with low CO content (ID-ref 100) and CO_2 reformate (CO_2-ref). The compositions are given in Table 1. The characteristic bands arising from the interaction with the respective reaction atmospheres are labeled in the spectra in Figs. 2, 4 and 5. Since the different characteristic bands and their assignment were discussed in detail previously [25], we will only summarize the assignment of the different signals at this point. On all four catalysts, we find characteristic signals in the CO_{ad} region at ~2000–2040 cm^{-1} and at 1980 cm^{-1}, depending on the CO content in the gas mixture, which are generally attributed to CO adsorbed in a linear or bridged configuration on the Ru NPs, respectively [24,35–43]. A signal at 2075 cm^{-1} was assigned previously to CO adsorbed on Ru^{n+} species [40,44]. The exact frequencies vary slightly with reaction conditions.

The OH region exhibits two peaks at 3740 and 3600 cm^{-1}, which we relate to silanol species and isolated structural or adsorbed OH groups on the support [45,46]. In CO_2-containing reformates, CO_2-related overtone signals (not marked) appear at 3450, 3540, 3600, 3640, 3700 and 3740 cm^{-1}, in addition to the OH-related signals in this region.

The CH_x spectral region shows the typical $CH_{x,ad}$ signals at 3016, 2928, and 2860 cm^{-1}, arising from gas phase CH_4, $CH_{3,ad}$, and the symmetric and asymmetric CH_2 vibrations on the respective catalysts [24,40,47]. A shoulder at ~2905 cm^{-1} was assigned to the CH vibration of a surface formate [11,48]. Depending on the catalyst and the reaction conditions, only some of the bands are resolved. At higher conversions, all of these bands are visible.

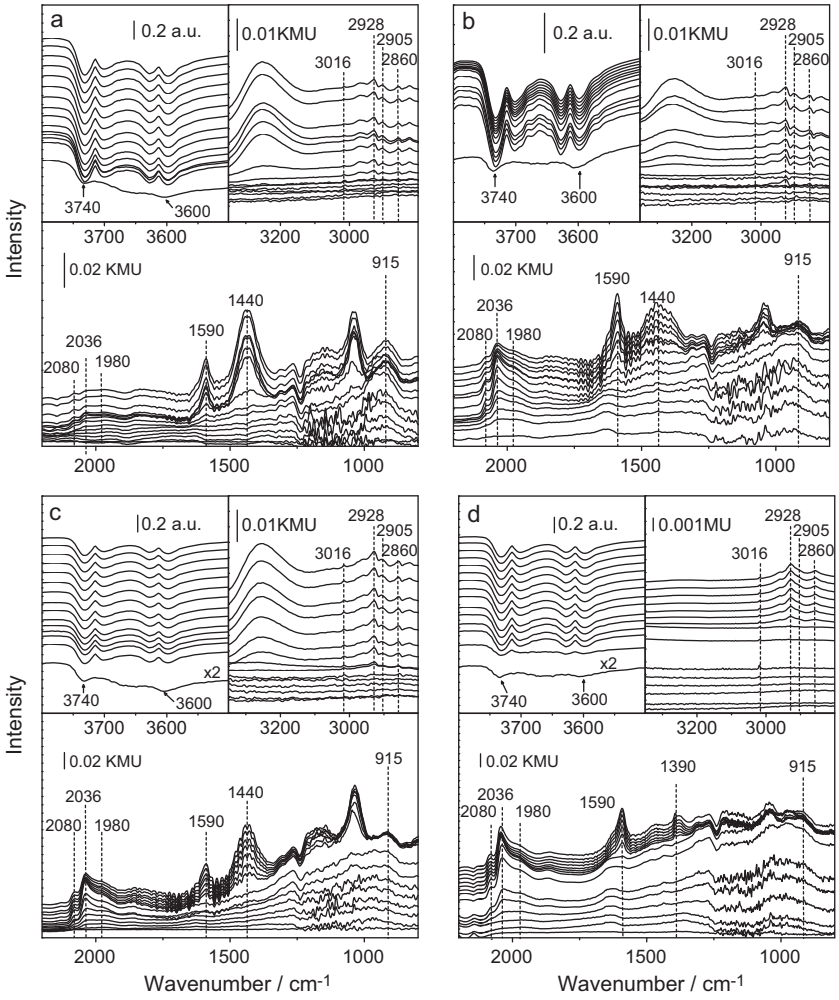

Fig. 2. DRIFT spectra recorded during 1000 min on stream at 190 °C on the Ru/zeolite catalysts in SR-ref 6000 reformate (a) 1.0 wt.% Ru/zeolite, (b) 2.2 wt.% Ru/zeolite, (c) 3.6 wt.% Ru/zeolite and (d) 5.6 wt.% Ru/zeolite; from bottom to top: 0, 2, 3, 5, 7, 15, 45, 105, 195, 345, 495, 645, 795, 915 min.

In the OCO region, bands at 1590, 1440, 1390 and 915 cm^{-1} were assigned to surface formates (1590 and 1390 cm^{-1}), carbonates (1440 cm^{-1}) and CH_2 vibrations (915 cm^{-1}) resulting from chain growth.

3.2.1. SR-ref 6000 reformate

In a first set of experiments, the temporal evolution of the different signals of the respective surface species on the 1.0 wt.%, 2.2 wt.%, 3.6 wt.%, and 5.6 wt.% Ru/zeolite catalysts in SR-ref 6000 ($CO/CO_2/H_2/N_2$) was investigated and characterized by sequences of *in situ* DRIFTS measurements (Fig. 2a–d) over 1000 min. The steady-state intensities of the CO_{ad} signal at ~2036 cm^{-1} after 1000 min of the CO_{ad} surface species are given in Table 3.

During reaction in SR-ref 6000 (Fig. 2a–d), we find for all four catalysts characteristic signals in the CO_{ad} region at ~2036 cm^{-1} (linear CO_{ad}) and 1980 cm^{-1} (bridged CO_{ad}) [24,36–43], and a signal at 2080 cm^{-1}, associated with CO adsorbed on oxidized Ru^{n+} or coadsorbed with O_{ad} on Ru [35,40,44]. After passing through a maximum after about 100 min, a constant level of the adsorbed CO_{ad} surface species is reached after ~500 min on all four catalysts. It should be noted that the CO_{ad} band intensity in SR-ref 6000 represents the maximum CO_{ad} intensity that can be reached on the respective catalysts. This was tested in measurements using reaction gas mixtures with higher CO concentrations, which yield similar band intensities. Accordingly, the CO_{ad} coverage must be at or close to saturation. The loss of the CO_{ad} signal intensity with time on stream, after having passed through the maximum, is most likely due to agglomeration of Ru NPs or deposition of deactivating carbon on the Ru surface as already discussed in Ref. [25].

In the OH region, CO_2-related overtone signals (not marked) appear at 3450, 3540, 3600, 3640, 3700 and 3740 cm^{-1}, in addition to the OH-related signals in this region, which blur the OH signals.

The CH_x spectral region shows the typical $CH_{x,ad}$ signals at 3016, 2928, and 2860 cm^{-1} [24,40]. On all four catalysts, these species (except CH_4) start to grow in after about 15 min on stream and reach a steady-state situation after 1000 min. For the CH_4 signal, steady-state is reached much faster, after about 10 min. A shoulder at ~2905 cm^{-1}, observed all on four catalysts, indicates the presence of C–H vibrations of surface formate species [11,48].

In the OCO region, bands at 1590, 1440 and 1390 cm^{-1}, related to surface formates (1590 and 1390 cm^{-1}) and carbonates (1440 cm^{-1}) [11], appear after about 100 min on stream on the four Ru/zeolite catalyst [38,48]. These bands grow steadily in intensity and do not saturate over 1000 min.

The steady-state CO_{ad} band intensity (Fig. 2a–d) increases with the amount of active metal deposited on/in the zeolite support, by factors of 2.7, 3.9 and ~5.6 (see Table 3), respectively, with increasing Ru loading. This is significantly more than the increase in Ru surface area, which increases by factors of 1.45, 2.04, and 2.81 (calculated from the average Ru particle size, Tables 2 and 3) in the same order (see Section 3.1 for the calculation of dispersion). Quantitative

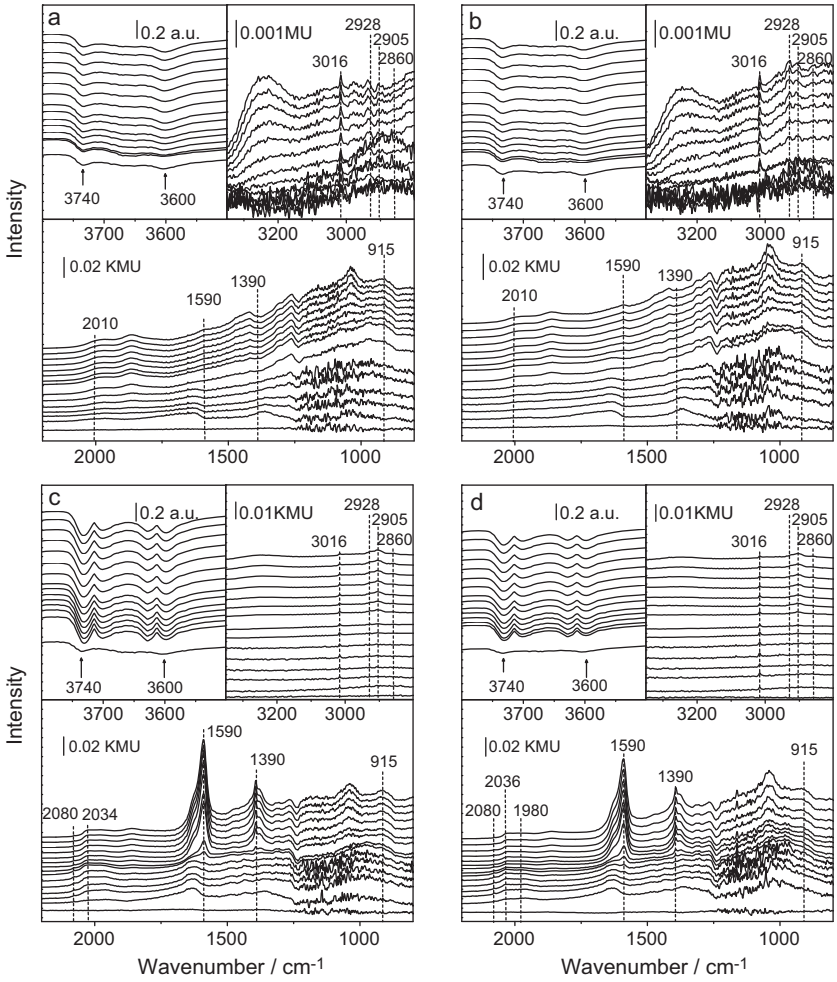

Fig. 3. DRIFT spectra recorded during 1000 min on stream at 190 °C over the Ru/zeolite catalysts; left panels: 3.6 wt.% Ru/zeolite, right panels: 5.6 wt.% Ru/zeolite in ID-ref 100 reformate (a, b), and SR-ref 100 (c, d); from bottom to top: 0, 2, 3, 5, 7, 15, 45, 105, 195, 345, 495, 645, 795, 915 min.

conclusions are hard to draw, however, because of the complex correlation between DRIFTS intensity (in KM units) and total amount of adsorbate molecules for the different catalysts, even if the support is identical. Since the CO_{ad} band intensity was shown earlier to be correlated with the methanation activity [25], the increase in CO_{ad} band intensities can be compared with that in catalytic activity (Section 3.3). Here it is most appropriate to compare with Ru surface area normalized rates, which are linearly correlated with the turnover frequencies. The latter increase by a factor of 4.4 for going from the 1 wt.% to the 5.6 wt.% Ru/zeolite catalyst.

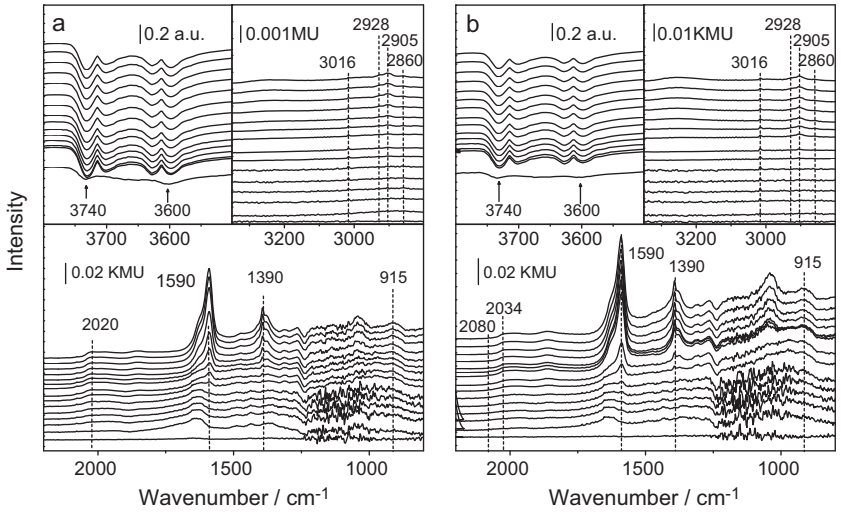

Fig. 4. DRIFT spectra recorded during 1000 min on stream at 190 °C over the Ru/zeolite catalysts (a) 3.6 wt.% Ru/zeolite catalyst, (b) 5.6 wt.% Ru/zeolite catalyst in CO_2-ref reformate; from bottom to top: 0, 2, 3, 5, 7, 15, 45, 105, 195, 345, 495, 645, 795, 915 min.

Table 3
CO_{ad} band intensity under steady-state conditions during CO methanation on the different catalysts in different reformates. CO_{ad} saturation intensity obtained in SR-ref 6000 relative to that of the 1 wt.% catalyst (2nd column), CO_{ad} intensity relative to saturation on the respective catalyst in semi-realistic reformate (SR-ref 6000) (subsequent columns, data for 2.2 wt.% catalyst from Ref. [26]).

Catalyst	Relative CO_{ad} saturation intensity	Ru surface area[a] /10^5 cm^2	ID-ref 100/%	SR-ref 100/%	CO_2-ref/%	SR-ref 6000/%
1 wt.% Ru/zeolite	1	0.53	–	–	–	100
2.2 wt.% Ru/zeolite	2.7	0.77	6	6	6	100
3.6 wt.% Ru/zeolite	3.9	1.08	9	10	10	100
5.6 wt.% Ru/zeolite	5.6	1.49	10	12	12	100

[a] With respect to 1 g of catalyst.

3.2.2. Reformate gases with low CO concentrations

In order to gain more information on the activity of the catalysts for CO_2 methanation, we conducted measurements in three reaction mixtures with low CO contents, SR-ref 100 (Fig. 3a, b), ID-ref 100 (Fig. 3c, d) and CO_2-ref (CO-free) (Fig. 4a, b), on the 3.6 wt.% (Figs. 3a, c and 4a) and the 5.6 wt.% (Figs. 3b, d and 4b) Ru/zeolite catalyst. Similar measurements on the 2.2 wt.% Ru/zeolite catalyst were already reported earlier [26], and the data will be used for comparison. For the 1 wt.% loaded catalyst, we expect a similar adsorption and reaction behavior as for the 2.2 wt.% catalyst.

The spectra obtained in these atmospheres (SR-ref 100, ID-ref 100 or CO_2-ref) do not differ significantly from the spectra discussed above in their general appearance. They differ, however, in the band intensities, especially of the $CH_{x,ad}$ and the CO_{ad} related signals, and their temporal evolution. Therefore, the band intensities of the linearly adsorbed CO_{ad} species on Ru obtained in the different reaction atmospheres are plotted vs. time in Fig. 5a–c for the 2.2 wt.%, the 3.6 wt.% and the 5.6 wt.% Ru/zeolite catalyst, respectively. The 2.2 wt.% Ru/zeolite catalyst was investigated earlier, the CO_{ad} intensities in Fig. 5a are taken from Ref. [26].

If, as proposed earlier [27,49,50], the methanation of CO_2 proceeds via CO_{ad} as reaction intermediate, the CO_{ad} band intensity can be taken as a measure of the CO_2 methanation activity in CO-free CO_2-ref, while in CO containing reformates the situation is more complex and both CO_2 decomposition and CO adsorption as well as the processes for CO_{ad} removal, CO_{ad} desorption and CO_{ad} methanation, contribute to the steady-state CO_{ad} coverage and band intensity. Therefore we have to compare the CO_{ad} band intensities in the different reformates, ID-ref 100, SR-ref 100, SR-ref 6000 and CO_2-ref, in order to gain more quantitative information about the physical origin of the CO selectivity. The same procedure was applied for a Ru/Al_2O_3 and the 2.2 wt.% Ru/zeolite catalyst recently [26], where the differences in the CO_{ad} band intensity obtained in the different reaction gas compositions (CO_2-ref, ID-ref 100 and SR-ref 100) and their correlation with the selectivity for CO methanation in the different semi-realistic reformates indeed allowed us to draw conclusions on the origin of the selectivity for CO methanation on these catalysts [26]. A similar approach will be used in the present study. It should be noted that a similar quantitative evaluation of the evolution of the $CH_{x,ad}$ related band intensities is not possible as these signals at 2926 cm^{-1} may be due to different surface species, CH_2 groups of carbon chains and $CH_{2,ad}$ as active intermediate for methanation.

The most important observations on the three catalysts are:

(i) In reaction atmospheres with low CO contents (ID-ref 100, SR-ref 100 and CO_2-ref (CO free); Figs. 3a–d and 4a, b), the final intensities of the CO_{ad} related signals are reached quickly within the first 100 min, as compared to ~800 min of the respective signals in reaction atmospheres with higher CO content (SR-ref 6000) (Fig. 5a–c).
(ii) The final intensities of the CO_{ad} related bands are significantly lower in atmospheres, with low CO contents, regardless of the presence of CO_2, and in CO_2-ref than in SR-ref 6000 for all catalysts. For the 2.2/3.6/5.6 wt.% Ru/zeolite catalysts, the final CO_{ad} band intensity in ID-ref 100 is only ~6/~9/~10% of that in SR-ref 6000, where the latter corresponds to saturation of the CO_{ad} band intensity (see Section 3.2.1). Hence, under these conditions, the Ru NPs are largely free of a reaction inhibiting CO adlayer and *per se* available for CO_2 methanation.
(iii) The effect of CO_2 in the gas-phase in low-CO (SR-ref 100) (Fig. 3a, b) or CO-free (CO_2-ref) (Figs. 4b, c and 5b, c) reformate depends sensitively on the catalyst loading. On the higher loaded 3.6 wt.% and 5.6 wt.% catalysts, the CO_{ad} band intensities in SR-ref 100 and CO_2-ref (CO-free) are ~10 and ~12% of the signal intensity in SR-ref 6000. The presence of CO_2 results in a clear increase in the CO_{ad} band intensity (relative to the intensity in a comparable CO_2-free atmosphere, ID-ref 100), indicating that the rate for CO_2 decomposition to CO_{ad} is of comparable order of magnitude as the rates for CO adsorption (from 100 ppm CO) and CO_{ad} desorption plus methanation, respectively, under present reaction conditions. Accordingly, exposure to CO_2-ref results in a CO_{ad} band intensity which is comparable to that obtained in SR-ref 100.

On the 2.2 wt.% Ru/zeolite catalyst [26], the situation is distinctly different (Fig. 5a). Addition of CO_2, by going from ID-ref 100 to SR-ref 100 reaction gas, does not increase the CO_{ad} signal intensity significantly. This implies that decomposition of CO_2 to CO_{ad} is slow compared to the rates for CO adsorption and CO_{ad} removal, by desorption plus CO_{ad} methanation, in SR-ref 100. Correspondingly, the CO_{ad} signal intensity resulting from exposure to CO_2-ref is much lower (~6%) than on the higher loaded Ru/zeolite catalysts and comparable to that obtained from direct adsorption of CO in 100 ppm CO containing atmosphere (exposure to ID-ref 100), which is also lower than on the higher loaded catalysts.

The above findings directly demonstrate that on the 2.2 wt.% Ru/zeolite catalyst CO_2 decomposition to CO_{ad} on the largely adsorbate-free Ru NPs is significantly slower than on the higher loaded catalysts with their larger Ru NPs, supporting our claim of an inherently slower CO_2 methanation rate on the former catalysts. Since these catalysts differ only in the Ru loading and in the Ru particle size, but not in the nature of the support, the differences in the CO_2 adsorption and CO formation behavior must be due to Ru particle size effects. This will be discussed in more detail in Section 3.3, after presentation of the catalytic activities.

3.3. Kinetic measurements

Fig. 6 illustrates the temporal evolution of the Ru mass normalized reaction rates of the 4 different Ru/zeolite catalysts in semi-realistic reformate ($CO/CO_2/H_2$) over 500 min. For all four catalysts, the reaction rate increases initially for about 100 min and stay constant afterwards. Table 4 summarizes the resulting final reaction rates. The results of the 2.2 wt.% catalyst closely resemble the data reported in earlier publications [25,26]. All catalysts show 100% CO selectivity under the present reaction conditions, which

Table 4
Activity (Ru mass normalized final rates) for CO methanation of the different catalysts in semi-realistic reformate (SR-ref 6000) and in low-CO semi-realistic reformate (SR-ref 100) (all columns: SR-ref 6000/SR-ref 100).

Catalyst	Reaction rate/ 10^{-6} mol[1] g_{Ru}^{-1} s^{-1}	Loading/ wt.% Ru	Relative reaction rate	Turnover frequency /10^{-3} s^{-1}	Relative TOFs	Selectivity %
1 wt.% Ru/zeolite	20/–	1/–	1	2.5[a]	1/–	100/–
2.2 wt.% Ru/zeolite	30/48	2.2	1.5/1	3.7/6.1	1.5/1	100/100
3.6 wt.% Ru/zeolite	36/50	3.6	1.8/1.04	8.0/11.2	3.2/1.8	100/90
5.6 wt.% Ru/zeolite	44/52	5.6	2.2/1.1	11.1/13.1	4.4/2.1	100/80

[a] The Ru particle size was assumed to be 0.9 nm, identical to the 2.2 wt.% catalyst.

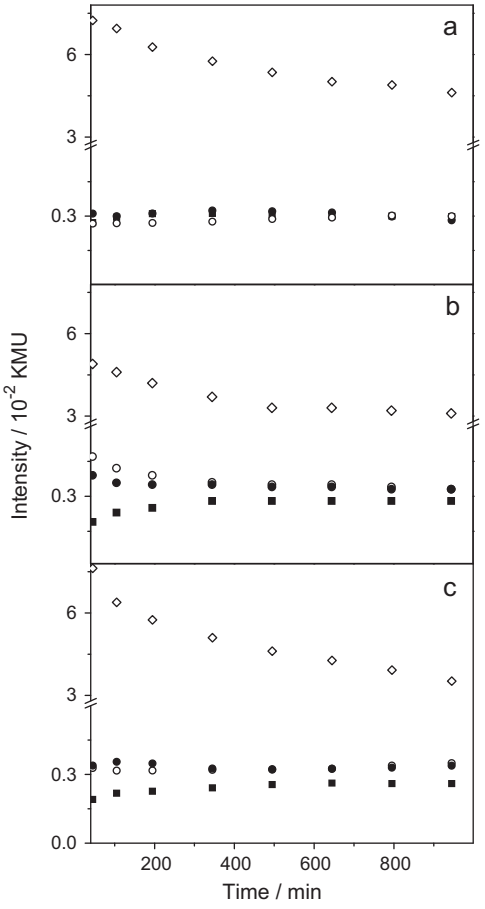

Fig. 5. Time evolution of the CO_{ad} band intensities (peak heights) obtained during reaction of the Ru/zeolite catalysts in different reaction atmospheres; (◊) SR-ref 6000, (○) SR-ref 100, (●) CO_2-ref, (■) ID-ref 100. (a) 2.2 wt.% Ru/zeolite catalyst, (b) 3.6 wt.% Ru/zeolite catalyst, (c) 5.6 wt.% Ru/zeolite catalyst.

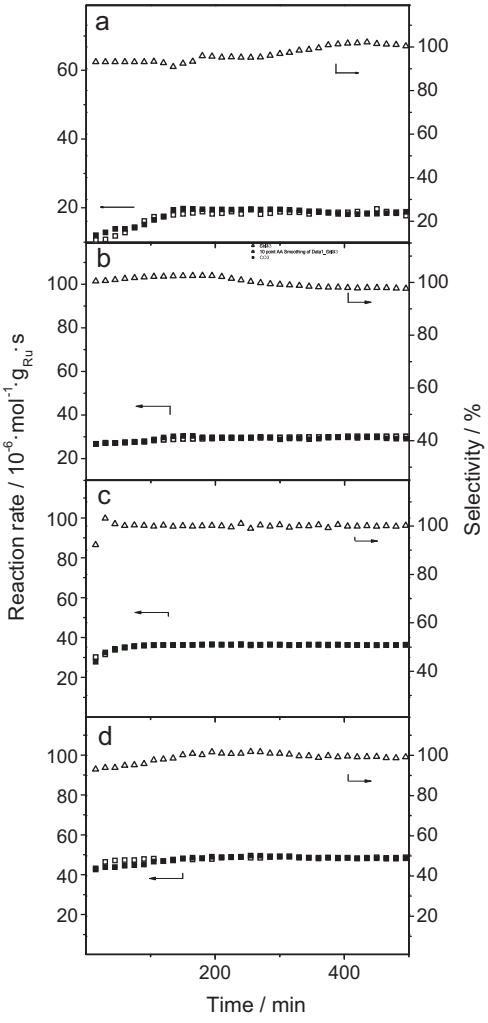

Fig. 6. Reaction rates and selectivities obtained for reaction over (a) the 3.6 and (b) the 5.6 wt.% Ru/zeolite catalyst (diluted with SiO_2) under differential reaction conditions in SR-ref 6000. (■) CO reaction rate, (□) CH_4 formation rate, (△) selectivity.

we mainly attribute to the fact that in the presence of 6000 ppm CO the surface of the Ru NPs is covered by a reaction inhibiting CO adlayer (the CO_{ad} band intensity is saturated under these conditions on all four catalysts, see Section 3.2.1), we explain the high selectivity for CO methanation under these conditions predominantly by a surface blocking effect, which prevents the decomposition of CO_2 to CO_{ad} and its further reaction to CH_4 (see also Ref. [26]). The higher CO methanation activity of all Ru/zeolite catalysts compared to the Ru/Al_2O_3 catalyst reported earlier [25,26] is attributed to strong metal support-interactions on the Ru/zeolite catalyst (see also below) [24,51]. Pronounced support effects on the CO methanation activity of Ru catalysts with comparable Ru particle sizes had been reported earlier [11,22]. Obviously, the Ru mass normalized reaction rate increases with increasing Ru content. A 5.6 fold increase of the Ru content (1–5.6 wt.% Ru) results in a 2.2 fold increase of the Ru mass normalized rate, and similar effects are observed also for the other two catalysts with intermediate loadings (see Table 4). This effect becomes even more pronounced when accounting for the lower fraction of surface atoms (dispersion) on the larger Ru NPs by using turnover frequencies, which are also listed in Table 4. (The TOFs are calculated assuming hemispherical Ru NPs of the mean particle size for the respective catalysts.) The TOF-based inherent activity of the Ru NPs increases by more than a factor of 4.4 from the 1 wt.% to the 5.6 wt.% Ru/zeolite catalyst. These trends in the CO methanation activity are also evident for reaction in low-CO reformate (SR-ref 100, see below and Fig. 7), where the mass based activity/TOF based activity increases by factors of ~1.1 and 2.14, respectively, when going from the 2.2 to the 5.6 wt.% catalyst. Hence, the intrinsic activity of the Ru/zeolite catalysts for CO

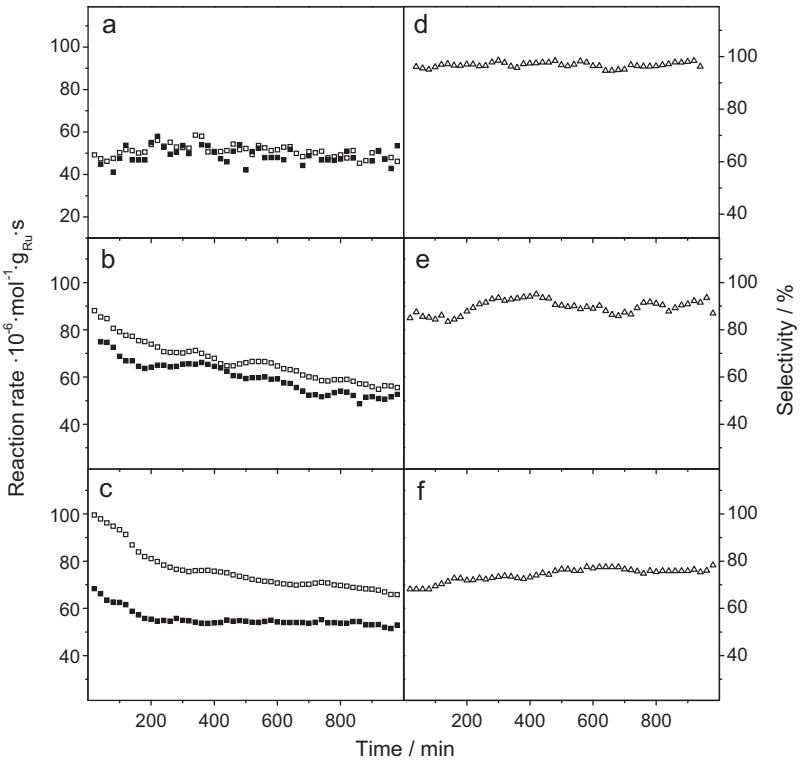

Fig. 7. Reaction rates (left panels) and selectivities (right panels) obtained for reaction over the 2.2 (a, d), 3.6 (b, e), and 5.6 wt.% (c, f) Ru/zeolite catalysts (diluted with SiO_2) under differential reaction conditions in SR-ref 100. (■) CO reaction rate, (□) CH_4 formation rate, (△) selectivity.

methanation increased significantly when higher catalyst loadings are used. Since there is no change in the nature of the support, we can unambiguously associate this with a particle size effect, leading to a higher activity of the larger Ru particles on the higher Ru loaded catalysts. This even overcompensates the loss of active Ru surface, as evident from the increase in Ru mass normalized reaction rates. In a microscopic picture, this trend can be understood by the increasing adsorption energy and metal–CO interaction of the CO_{ad} when going from smaller to larger particles (see Section 3.2), which leads to weakening of the C–O bond due to increasing population of the antibonding $2\pi^*$ orbital [52]. The increase in CO_{ad} adsorption energy is evident from the much lower intensity of the CO_{ad} band and CO_{ad} coverage under steady-state conditions in ID-ref 100 on the 2.2 wt.% catalysts (6% of I_{max}) as compared to the higher loading catalysts (3.6 and 5.6 wt.%: 9% and 10%, respectively, of I_{max}).

A similar trend of the particle size dependent CO methanation activity was reported in early studies by King [12], Kellner and Bell [13] and Che and Bennett [14] for reaction on differently loaded Ru/Al_2O_3 catalyst (1–11 wt.% Ru) under Fischer-Tropsch reaction conditions ($CO:H_2 = 1:2$). The dispersion of the Ru NPs was determined by H_2 chemisorption, yielding values between 30% and 90%. Hence, the Ru NPs on these catalysts are clearly smaller than those on the Ru/Al_2O_3 catalyst investigated in our laboratory previously (5 wt.% Ru, dispersion 15%) [25]. Especially at very high dispersions (>80%) the turnover frequencies were found to decrease dramatically. The above authors explained this by a structural effect, assuming that the methanation of CO requires crystallite faces whose amount increases with increasing particle size. For comparison, van Hardeveld and Hartog calculated that the fraction of terrace surface atoms (relative to all surface atoms) increases by a factor of 2 when increasing the particle size from 1.0 to 2.0 nm [54]. Comparable particle size effects were reported also for Ru catalysts on different supports in the ammonia synthesis [55], which these authors attributed to a higher number of B_5 adsorption sites on (1 1 0) facets on larger Ru NPs than on smaller ones. The support was proposed to play an important role by stabilizing certain Ru particle shapes. Similar effects would be reasonable also for the present systems, for zeolite and Al_2O_3 supported Ru catalysts in the selective CO methanation reaction.

More recent studies investigated the influence of the dispersion on the CO methanation reaction under conditions relevant for feed gas purification [10,19,22]. Although the mechanistic understanding is hampered by the fact that these studies were either performed under integral reaction conditions [22], or the CO_2 and CO methanation were investigated separately at different temperatures under differential reaction conditions [10], the results of these studies agree well with the findings of the early studies [12–14] and of our present work in the sense that they also observed an increasing activity with increasing particle size and higher Ru loading.

In the context of the present work, particle size effects on the selectivity are even more interesting than size related variations in the CO methanation activity. Previously, we demonstrated that the 2.2 wt.% Ru/zeolite catalyst exhibits a high CO methanation selectivity even at 100 ppm CO concentration in the presence of 15.5% CO_2, whereas the selectivity of a 5 wt.% Ru/Al_2O_3 catalyst (~2.5 nm Ru particle size) was rather low under similar reaction conditions [26]. We proposed that the small Ru particles of the Ru/zeolite catalyst are responsible for the high selectivity. In order to test such kind of particle size effects without interference with possible variations in the metal-support interactions, we performed CO methanation experiments in low-CO semi-realistic reformate (SR-ref 100, 0.01% CO, 15.5% CO_2, rest H_2) on the 3.6 wt.% and on the 5.6 wt.% Ru/zeolite catalysts with their larger Ru particle sizes, similar to the previous measurement on the 2.2 wt.% Ru/zeolite catalyst [26]. Fig. 7a–c depict the CO methanation and the CH_4 production rate on the 2.2 wt.%, the 3.6 wt.% and the 5.6 wt.% Ru/zeolite catalysts, whereas Fig. 7d–f show the selectivity for CO methanation. The 3.6 wt.% catalyst exhibits a CO methanation rate of 50×10^{-6} mol g_{Ru}^{-1} s^{-1} and a CO methanation

selectivity of 90%, whereas for the 5.6 wt.% catalyst the corresponding values are 52×10^{-6} mol g_{Ru}^{-1} s^{-1} and 80%. For the 2.2 wt.% catalyst, we had determined values of 48×10^{-6} mol g_{Ru}^{-1} s^{-1} and 100% [26]. The higher reaction rates compared to reaction in the SR-ref 6000 reformate (0.6% CO) are due to the lower CO concentrations (0.01%), reflecting the negative CO reaction order reported in [26].

The observed decay in selectivity with increasing Ru particle size agrees well with the trends in the CO_{ad} signal intensities in the DRIFTS measurements, where the difference between reaction in ID-ref 100 and SR-ref 100 increases from essentially zero (2.2 wt.%) via 1% of the saturation intensity (3.6 wt.%) to 2% of the saturation intensity (5.6 wt.%) (note that the error margins are below 1%), and where the CO_{ad} intensity in CO_2-ref increases from 6% to 12% of the saturation intensity in the same order (Table 3). These trends fully agree also with our previous proposal for the physical origin of the selectivity for CO methanation on Ru/zeolite catalysts [26]. The very small particles dominant on the lower loaded Ru/zeolite catalysts (1 wt.% and 2.2 wt.%) are little active for CO formation from reversibly adsorbing CO_2, as indicated by the lower CO_{ad} band intensity observed in CO-free CO_2-reformate as compared to the higher loading Ru/zeolite catalysts. (For the 1 wt.% catalyst we assume similar or lower particle sizes as on the 2.2 wt.% catalyst based on the adsorption/reaction characteristics.) This is attributed to a higher barrier for CO_2 dissociation, which, according to the Brønstedt–Evans–Polanyi relation [56,57], agrees perfectly with the weaker CO adsorption, derived from the decreasing CO_{ad} band intensity on these catalysts in Ref. [26]. Hence, on these catalysts, the high selectivity for CO methanation even at low CO concentrations is driven by an inherently low activity for CO_2 methanation, due to a higher barrier for CO formation from reversibly adsorbed CO_2. Of course, at higher CO concentrations site blocking by a closed CO adlayer comes as an additional effect.

For the higher loading Ru/zeolite catalysts we had assumed that their larger mean Ru particle sizes (3.6 wt.%: 1.6 nm, 5.6 wt.%: 1.9 nm) results from a coexistence of larger Ru NPs outside the zeolite particles and very small Ru NPs (0.8–0.9 nm diameter) inside the pores, as present on the low loading catalysts. On the larger Ru NPs, the selectivity is proposed to be controlled by a site blocking mechanism, where the active Ru surface is essentially covered by strongly adsorbed CO_{ad}, preventing the dissociative adsorption of CO_2, which corresponds to the previous ideas for the origin of the selectivity in the selective CO methanation over Ru catalysts [17,18]. As the CO concentration and hence the CO_{ad} coverage decreases, CO_2 can adsorb on the resulting empty sites and dissociate to CO_{ad}, which acts as intermediate for the CO_2 methanation [27,49,50]. Therefore, the selectivity for CO methanation decreases with decreasing CO concentration in the feed gas. The very small Ru NPs (in the zeolite pores), which are most likely present also on these catalysts, behave similarly as on the low loading Ru/zeolite catalysts, with an inherently lower activity for CO_2 dissociation to CO_{ad}. On a microscopic scale, this trend towards a higher inherent activity for larger Ru particles can again be explained by in terms of the Brønstedt–Evans–Polanyi relation, similar to the correlation between CO methanation rate and CO_{ad} adsorption energy, where larger Ru particles result in a higher CO methanation rate and a higher CO adsorption energy. A similar correlation is likely also between CO_{ad} stabilization and CO_2 decomposition, where stabilization of CO_{ad} (increasing particle size) should be correlated with an increase in CO_2 decomposition (stabilization of the final state and of the transition state), in agreement with experimental findings.

Based on the above trends, the variation in the selectivity for CO methanation on the different Ru/zeolite catalysts is dominated and can be rationalized consistently by particle size effects. This may be different when changing the nature of the support. We had demonstrated above that particle size effects are not sufficient to rationalize the different activities of the Ru/zeolite catalysts and a Ru/Al_2O_3 catalyst with larger Ru NPs (~2.5 nm). Also, for the 5.6 wt.% Ru/zeolite catalysts, whose mean particle size is not so different from that of the Ru/Al_2O_3 catalyst, the Ru mass based activity differs by more than one order of magnitude from that of the latter one. (Extrapolating from lower loaded Ru/zeolite catalysts with smaller Ru NPs this difference should even increase when going to hypothetical Ru/zeolite catalysts with even larger Ru NPs (~2.5 nm).) Similar discrepancies are also observed for the inherent activity for CO_2 methanation, which controls the selectivity at low CO concentrations. We reported recently that exposure of the Ru/Al_2O_3 catalyst to CO_2-ref under identical reaction conditions results in a similar CO_{ad} band intensity as obtained in SR-ref 6000, which in turn corresponds to the maximum intensity achieved on this catalyst (CO_{ad} saturation) [26]. In contrast, on the 5.6 wt.% Ru/zeolite catalyst, this value was only 12% of the saturation intensity. Hence, on the Ru/Al_2O_3 catalyst with its larger Ru NPs (~2.5 nm particle size), CO_2 decomposition is relatively fast compared to the combined rates of CO_{ad} desorption and CO_{ad} methanation on that catalyst. On the other hand, we have to consider that on the Ru/Al_2O_3 catalyst also the methanation of the resulting CO_{ad} was much slower, by at least one order of magnitude, than on the 5.6 wt.% Ru/zeolite catalyst (see above and Ref. [26]), which leads to a higher CO_{ad} steady-state coverage on Ru/Al_2O_3 in CO_2-ref than on the 5.6 wt.% Ru/zeolite catalyst for a similar CO_2 decomposition rate. Hence, metal-support interactions affect also the CO_2 methanation reaction and hence the selectivity, either indirectly via the build-up of a reaction inhibiting CO adlayer, via the competition between CO_{ad} formation from CO_2 and CO_{ad} removal, or directly.

Finally, we want to briefly comment on the implications of these findings for technical application, i.e., for CO removal from CO-contaminated feed gases for low-temperature polymer electrolyte fuel cells (PEFCs). Obviously, both processes for removal of small amounts of CO (<1%), the preferential oxidation of CO (PROX) and the selective methanation of CO (SelMeth) are facing limitations in the down-stream part of the reactor with its low residual CO concentrations, if the selectivity is only due to reaction inhibiting CO adlayer on the active particles. This leads to considerable H_2 consumption due to H_2 oxidation (PROX reaction) or due to CO_2 methanation (SelMeth reaction) The much simpler technical realization of the SelMeth reaction as compared to a PROX reactor, makes this pathway attractive from a technical point of view. Therefore, catalysts with an inherently low activity for H_2 oxidation (PROX reaction) or, as in the present case, for CO_2 methanation (SelMeth reaction) are ideal candidates for complete CO removal from these fuels, and fundamental for the realization of the SelMeth process.

For reaction in the regime of very low CO contents, at the end of the catalyst bed in technical applications, only inherently low activities for CO_2 decomposition will maintain the high selectivities of ~100%, which can be obtained via the site blocking mechanism at higher CO concentrations in the reformate gas mixture. This is crucial for the implementation of the Selective Methanation as a technically simple and therefore attractive technology for fine purification of H_2-rich feed gases for low-temperature PEFCs, which were prepared by steam reforming of fossil fuels and therefore contain large amounts of CO_2 in addition to CO impurities.

4. Conclusion

We have systematically investigated the effect of Ru loading and of the Ru particle size on the reaction behavior of differently loaded Ru/zeolite catalysts in the selective methanation of CO in CO_2-rich reformate gases, employing *in situ* XAS, *in situ* DRIFTS and kinetic measurements in reformate gases with different CO

contents. Combining the structural information (particle sizes) from XAS measurements, the time-resolved information on the build-up of the adlayer and in particular of the CO_{ad} coverage on the different catalysts and in different reaction atmospheres from DRIFTS measurements, and the trends in reactivities and selectivities for CO methanation obtained from the kinetic measurements, we arrived at the following conclusions on the reaction behavior of these Ru/zeolite catalysts:

1. The Ru particle size, measured by XAS under steady-state conditions in idealized reformate, is clearly correlated with the Ru loading; it increases from 0.9 nm for the 2.2 wt.% catalyst to 1.9 nm for the 5.6 wt.% catalyst. We propose that (i) the small Ru NPs are located in the pores of the zeolite, and that (ii) for the higher loading catalyst both 0.9 nm Ru NPs in the pores of the zeolite and larger Ru NPs on the outer surface of the zeolite particles coexist. The 1 wt.% catalyst we expect to closely resemble the 2.2 wt.% catalyst, with very small Ru NPs in the pores of the zeolite.
2. The activity of the Ru/zeolite catalysts for CO methanation (both TOF-based activity and Ru mass normalized rates) increases with increasing Ru particle size. Since variations in the metal-support interactions can be excluded, the changes in reactivity purely reflect a particle size effect. In addition, the rates are significantly higher, by at least a one order of magnitude, than for a Ru/Al_2O_3 catalyst under identical reaction conditions and extrapolated to similar particle sizes. This difference must be solely due to a variation in the metal-support interaction.
3. The adsorption energy of CO_{ad} increases with increasing Ru particle size, as evident from the increasing relative CO_{ad} band intensity and hence increasing CO_{ad} coverage in low-CO idealized reformate under identical adsorption/reaction conditions. In reformate gas with higher CO concentrations, the CO_{ad} band intensity reaches its saturation level, independent of catalyst loading/Ru NP size.
4. In the absence of CO, the dissociation rate for CO_2 increases with increasing Ru particle size, as indicated by the increasing CO_{ad} band intensity This leads to an increasing inherent activity for CO_2 methanation with increasing Ru particle size. In good agreement with the increasing activity for CO_2 decomposition, its contribution to the CO_{ad} band intensity in low-CO reformate with Ru loading/NP size, as evident from comparison with the band intensity in the same atmosphere, but without CO_2.
5. In low-CO reformate, the CO selectivity decreases with increasing Ru NP size, from 100% for the 2.2 wt.% catalyst to 80% for the 5.6 wt.% Ru/zeolite catalyst. In contrast, in reformate gas with higher CO concentration, the CO selectivity is constant at 100%, independent of catalyst loading/Ru NP size.
6. The high selectivity for CO methanation of the Ru/zeolite catalysts and its particle size dependence are explained by a combination of two effects: (i) a site blocking mechanism, where a reaction inhibiting, strongly bound CO adlayer blocks the decomposition of CO_2 to CO_{ad} and its further methanation, as it was proposed for Ru catalysts earlier and (ii) a decreasing inherent activity for CO_2 dissociation to CO_{ad} with decreasing Ru particle size. The former results in a high selectivity at higher CO concentrations, independent of the Ru particle size, while the latter is responsible for the very high selectivities obtained even at very low CO concentrations, despite the presence of vast amounts of CO_2. The pronounced decrease in activity for CO_2 dissociation for very small Ru particles is explained in terms of the Brønstedt–Evans–Polanyi relation, with the barrier for CO_2 dissociation increasing with a decrease of the CO_{ad} adsorption energy at decreasing Ru particle size.
7. In addition to particle size effects, also metal-support interactions play a role and affect the selectivity for CO methanation of the Ru/zeolite catalysts, as evident from the much higher selectivity of the highest loading Ru/zeolite than the Ru/Al_2O_3 catalyst with comparable particle sizes in low-CO reformate. Metal support interactions may affect the selectivity either directly, via the activity for CO_2 decomposition, or indirectly, by modifying the ratio between CO_{ad} formation and CO_{ad} removal (desorption plus methanation), which changes the steady-state coverage of the reaction inhibiting CO adlayer.

Acknowledgements

We would like to thank the group of J. van Bokhoven (ETH Zürich) for many helpful discussions on XAS related topics, and Hasylab and ESRF for providing beam time at stations X1 and BM26, respectively.

Appendix A. Supplementary data

Supplementary data associated with this article can be found, in the online version, at doi:10.1016/j.cattod.2011.08.035.

References

[1] J.R. Rostrup-Nielsen, K. Aasberg-Petersen, in: W. Vielstich, H.A. Gasteiger, A. Lamm (Eds.), Fuel Cell Technology and Applications, vol. 3, 1st ed., Wiley, Chichester, 2003 (Chapter 14).
[2] S. Kawatsu, J. Power Sources 71 (1998) 150.
[3] D.L. Trimm, Z.I. Önsan, Catal. Rev. 43 (2001) 31.
[4] R.M. Navarro, M.A. Pena, J.L.G. Fierro, Chem. Rev. 107 (2007) 3952.
[5] D.R. Palo, R.A. Dagle, J.D. Holladay, Chem. Rev. 107 (2007) 3992.
[6] M. Echigo, T. Tabata, J. Chem. Eng. Jpn. 37 (2004) 75.
[7] G.A. Mills, F.W. Steffgen, Catal. Rev. Sci. Eng. 8 (1974) 159.
[8] M.A. Vannice, J. Catal. 37 (1975) 449.
[9] L. Caldwell, Council for Scientific and Industrial Research 660 5 2, Selectivity in Fischer-Tropsch Synthesis, 1980.
[10] Z. Kowalczyk, K. Stolecki, W. Rarog-Pilecka, E. Miskiewicz, E. Wiczkowska, Z. Karpinski, Appl. Catal. A 342 (2008) 35.
[11] R.A. Dalla Betta, M. Shelef, J. Catal. 48 (1977) 111.
[12] D.L. King, J. Catal. 51 (1978) 386.
[13] C.S. Kellner, A.T. Bell, J. Catal. 75 (1982) 251.
[14] M. Che, C.O. Bennet, Adv. Catal. 36 (1989) 55.
[15] K. Asakura, Y. Iwasara, J. Chem. Soc. Faraday Trans. I 86 (1990) 2657.
[16] P. Panagiotopoulou, D.I. Kondarides, X.E. Verykios, Appl. Catal. A 344 (2008) 45.
[17] T. Inui, M. Funabiki, Y. Takegami, Ind. Eng. Chem. Prod. Res. Dev. 19 (1980) 385.
[18] M.B.I. Choudhury, S. Ahmed, M.A. Shalabi, Appl. Catal. A 314 (2006) 47.
[19] P. Panagiotopoulou, D.I. Kondarides, X.E. Verykios, Appl. Catal. B 88 (2009) 470.
[20] M. Krämer, M. Duisberg, K. Stöwe, W.F. Maier, J. Catal. 251 (2007) 410.
[21] M. Krämer, K. Stöwe, M. Duisberg, F. Müller, M. Reiser, S. Sticher, W.F. Maier, Appl. Catal. A 369 (2009) 42.
[22] A.R. Dagle, Y. Wang, G.-G. Xia, J.J. Strohm, J. Holladay, D.R. Palo, Appl. Catal. A 326 (2007) 213.
[23] D.J. Elliott, J.H. Lunsford, J. Catal. 57 (1978) 11.
[24] S. Scirè, C. Crisafulli, R. Maggiore, S. Minico, S. Galvagno, Catal. Lett. 51 (1998) 41.
[25] S. Eckle, Y. Denkwitz, R.J. Behm, J. Catal. 269 (2010) 255.
[26] S. Eckle, H.-G. Anfang, R.J. Behm, Appl. Catal. A 391 (2011) 325.
[27] S. Eckle, H.-G. Anfang, R.J. Behm, J. Phys. Chem. C 115 (2011) 1361.
[28] D.C. Koningsberger, B.L. Mojet, G.E. van Dorssen, D.E. Ramaker, Top. Catal. 10 (2000) 143.
[29] M. Vaarkamp, J.C. Linders, D.C. Koningsberger, Physica B 208–209 (1995) 159.
[30] A.L. Ankudinov, B. Ravel, J.J. Rehr, S.D. Conradson, Phys. Rev. B 58 (1998) 7565.
[31] I.M. Hamadeh, P.R. Griffiths, Appl. Spectrosc. 41 (1987) 682.
[32] F. Meunier, D. Reid, A. Goguet, S. Shekhtman, C. Hardacre, R. Burch, W. Deng, M. Flytzani-Stephanopoulos, J. Catal. 247 (2007) 269.
[33] K.I. Pandya, S.M. Heald, J.A. Hriljac, L. Petraskis, J. Fraissard, J. Phys. Chem. 100 (1996) 5070.
[34] A.M. Karim, V. Prasad, G. Mpourmpakis, W.W. Lonergan, A.I. Frenkel, J.G. Chen, D.G. Vlachos, J. Am. Chem. Soc. 191 (2009) 12230.
[35] R.D. Gonzalez, M.F. Brown, J. Phys. Chem. 80 (1976) 1731.
[36] A.A. Davydov, A.T. Bell, J. Catal. 49 (1977) 332.
[37] F. Solymosi, J. Raskó, J. Catal. 15 (1989) 107.
[38] E. Guglielminotti, G.C. Bond, J. Chem. Soc. Faraday Trans. I 86 (1990) 979.
[39] N.M. Gupta, V.S. Kamble, R.M. Iyer, T. Ravindranathan, M. Grätzel, J. Catal. 137 (1992) 473.
[40] M.W. McQuire, C.H. Rochester, J. Catal. 141 (1993) 355.
[41] K. Yokota, M. Fukui, T. Tanaka, Appl. Surf. Sci. 121/122 (1997) 273.
[42] N.M. Gupta, V.P. Londhe, V.S. Kamble, J. Catal. 169 (1997) 423.
[43] S.Z.H. Todorova, G.B. Kadinov, Res. Chem. Intermed. 28 (2002) 291.
[44] F. Solymosi, A. Erdöhelyi, T. Bansagi, J. Catal. 68 (1981) 371.

[45] H. Knözinger, P. Ratnasamy, Catal. Rev. 17 (1978) 31.
[46] S.T. Yong, K. Hidajat, S. Kawi, J. Power Sources 131 (2004) 91.
[47] J.G. Ekerdt, A.T. Bell, J. Catal. 58 (1979) 170.
[48] N.M. Gupta, V.S. Kamble, V.B. Kartha, R.M. Iyer, K.R. Thampi, M. Gratzel, J. Catal. 146 (1994) 173.
[49] M.R. Prairie, A. Renken, J.G. Highfield, K.R. Thampi, M. Grätzel, J. Catal. 129 (1991) 130.
[50] I.A. Fisher, A.T. Bell, J. Catal. 162 (1996) 54.
[51] R.J. Davis, J. Catal. 216 (2003) 396.
[52] O.R. Inderwildi, S.J. Jenkins, D.A. King, J. Phys. Chem. C 112 (2008) 1305.
[54] R. van Hardeveld, F. Hartog, Surf. Sci. 15 (1969) 189.
[55] C.J.H. Jacobsen, S. Dahl, P.L. Hansen, E. Törnqvist, L. Jensen, H. Topsøe, D.V. Prip, P.B. Møenshaug, I. Chorkendorff, J. Mol. Catal. A 163 (2000) 19.
[56] N. Brønstedt, Chem. Rev. 5 (1928) 231.
[57] M.G. Evans, N.P. Polanyi, Trans. Faraday Soc. 34 (1938) 11.